

Evaluation of the Effects of Length on Strength of Slender Pillars in Limestone Mines Using Numerical Modeling

Dennis R. Dolinar, Lead Research Engineer
Gabriel S. Esterhuizen, Senior Research Engineer
NIOSH-Pittsburgh Research Laboratory
Pittsburgh, PA

ABSTRACT

In this National Institute for Occupational Safety and Health (NIOSH) investigation, numerical modeling is used to evaluate the degree the pillar strength is increased with a rectangular pillar over a square pillar. Three-dimensional models are developed with pillar sizes and geometries typical of underground limestone mines in the United States. Physical properties for the models are based on geotechnical surveys of nearly 30 underground limestone mines. To examine the effects of pillar length on pillar strength with the modeling, a parametric study was conducted where the pillar width was held constant while the length and height were varied resulting in width-to-height ratios ranging from 0.5 to 1.5 and width to length ratios ranging from 1 to 6.

There are two aspects to pillar strength and failure. At relatively low stresses, pillars can fail as a result of geologic structure. At greater depths and sufficient extraction ratios, the pillars can also fail as a result of the vertical stresses exceeding the pillar strength. The effects of increasing pillar length regarding both strength aspects are presented in this study.

Equations were developed for the increase in pillar strength with both height and length based on the model results. The results from these equations were compared to those from previously developed empirical equations for rectangular pillars. For the more slender limestone pillars with a width-to-height ratio below one, there is little increase in pillar strength for length-to-width ratios above 2 and almost no increase with length for a width-to-height ratio of 0.5. Only with the more squat pillars is there a significant improvement in strength with length. The gain in pillar strength with length for the pillars is explained by the change in the ratio of the area of the pillar affected by the ends to the area of the pillar. For the squattest pillar, the change in strength is also affected by an increase in pillar confinement along the central length of the pillar as the pillar transitions from a square to a long rectangular pillar. With geologic structure, added pillar length can significantly improve the pillar strength, depending on the strike of that structure with respect to the long pillar axis.

INTRODUCTION

This investigation was conducted as part of an effort to improve safety in underground limestone mines by evaluating and improving the performance of the pillars. Highly stressed pillars that are approaching failure have an increased potential for spalling and fall of material from the ribs; thus increasing the hazard of ground fall injuries to workers while pillar failure can impact operations. In this investigation, the effects on pillar strength of the pillar length are evaluated. There are two aspects to pillar strength and failure. At relatively low stresses, pillars can fail as a result of geologic structure (Esterhuizen et al., 2006; Iannacchione and Coyle, 2002). A detailed analysis of the strength reduction of square limestone pillars with geological weaknesses has previously been conducted (Iannacchione, 1999). The analysis did not include the effects of pillar length. However the following comment was made about rectangular pillars “The orientation of a discontinuity is important when the pillars are rectangular in that the strength will be affected most if the discontinuity is aligned with the long axis of the pillar.” At greater depths and sufficient extraction ratios, the pillars can also fail as a result of the vertical stresses exceeding the pillar strength. The effects of increasing pillar length regarding both strength aspects will be presented in this study.

Rectangular pillars have been used in situations where horizontal stress is an issue. Through the use of rectangular pillars, the roof exposed to failure from the maximum horizontal stress can be minimized (Iannacchione et al, 2003). Longer pillars can also increase the efficiency of ventilation in the limestone mines (Grau et al., 2002 and 2006). With longer pillars, the number of ventilation stoppings can be reduced. However, this study is designed to determine to what degree the pillar strength can be increased by using rectangular pillars over the more standard square pillars. The approach in this study is to use numerical modeling to evaluate the effects of pillar length on the pillar strength. There have been a number of equations developed to predict the increase in strength from a square to a rectangular pillar. Many of these equations have not been substantiated, or have been used for coal pillars which are much squatter pillars than used in limestone. The pillar sizes and geometries used in the models are typical of underground limestone mines in the United States.

BACKGROUND

There have been a number of equations proposed for the increase in pillar strength with length. These include the Bauschinger-Johnson, Mark-Bieniawski, Grobbelaar and Wagner equations (Babcock, 1994; Mark and Chase, 1997; Mark 1999; Salamon, 1983). These equations were developed using either an intuitive, empirical, or analytical approach or a combination of these approaches. Figure 1 shows the strength increase over a square pillar from these equations for two fairly small width-to-height ratios. The equations obviously give somewhat different results, although all the equations indicate that the rate of increase in pillar strength diminishes as the pillar length increases.

The Bauschinger-Johnson equation was developed to a large extent from laboratory testing. This experimental work formed the basis of the effects of the width-to-height ratio that other researchers have developed for pillar design in both coal and hard rock mines. However, based on figure 1, the results of this equation are not relevant for a width to height ratio of 0.5, a ratio that is seen in benched areas of limestone mines. This ratio appears to fall outside the range of the experimental data used to develop the equation.

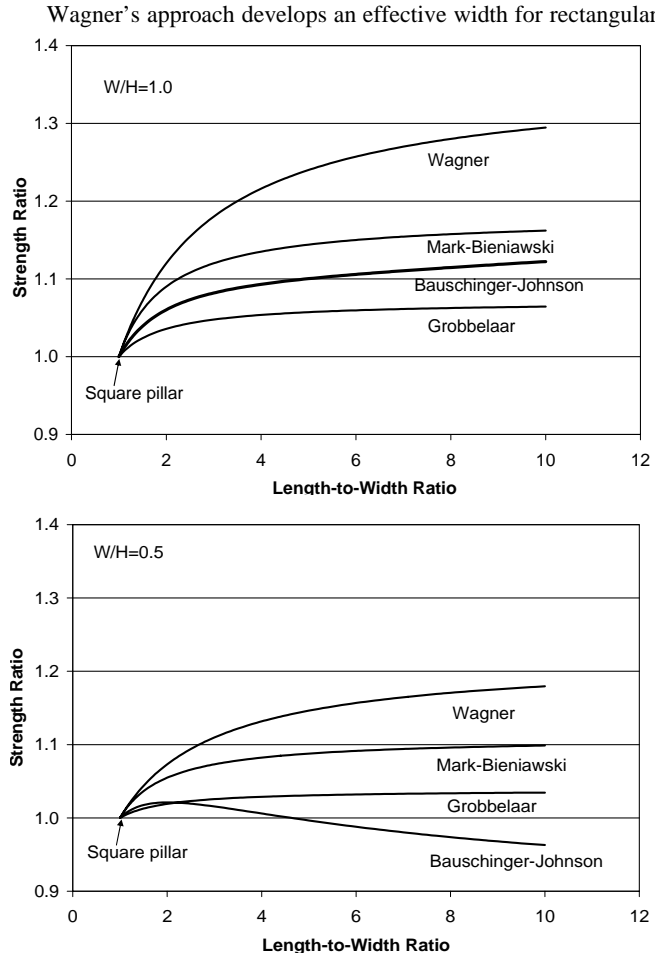


Figure 1. The ratio of the compressive strength of various rectangular geometries compared to a square pillar from four different pillar equations (Babcock, 1994; Mark and Chase, 1997; Mark 1999; Salamon, 1983). (Top charts shows pillar width-to-height ratio equal to 1.0. Bottom charts shows pillar width-to-height ratio equal to 0.5).

pillars based on the pillar area and perimeter that can then be input into equations for pillar strengths that use a width-to-height ratio. For an infinitely long pillar, the effective width is twice that of a square pillar. Grobbelaar developed a rather complex analytical approach to pillar design. However, the equations can be simplified to develop an equation with the effects of length included. The Grobbelaar and Wagner equations or approaches have not been proven or substantiated (Roberts et al., 2005)

The Mark-Bieniawski equation is based on the Bieniawski formula for square pillars with an analytical analysis for load distribution in the pillar at peak load used to develop an equation for rectangular pillars. However, the constants and parameters in this equation are related to squat pillars in coal. Both equations form the basis of determining the pillar strength in both ALPS (Analysis of Longwall Pillar Stability) and ARMPS (Analysis of Retreat Mining Pillar Stability), which have been used in coal pillar design and are empirically developed from actual case studies of the performance of pillars (Mark, 1990; Mark and Chase, 1997; Mark, 1999).

For underground limestone, the pillars are very slender compared to those used in underground coal mines. On development, the pillars may be 8 m high by 12 m wide resulting in a width-to-height ratio of 1.5. With first bench mining, the height can be 12 m resulting in a width-to-height ratio reaching one. With multiple benches, the pillar can reach 24 m in height or greater, resulting in a width-to-height ratio of 0.5 or less.

Another consideration for limestone mines is the type of failure that can occur in these high openings with slender pillars. It has been noted in hard rock mines that pillar spalling and failure occur at stress levels well below the expected rock and pillar strength (Stacey and Yathavan, 2003). This has been attributed to brittle failure that can develop where the confining stresses are low and the geometry does not constrain crack growth. The application of brittle failure considerations to rectangular pillar design and performance will be discussed.

MODEL FAILURE CRITERIA

For modeling, an appropriate failure criteria must be selected along with the compatible properties that can produce realistic results. Pillars in hard rock mines, including limestone, will typically slab and split at stresses that are only 0.04 to 0.35 of the uniaxial compressive strength of the intact rock (Stacey and Yathavan, 2003). This is thought to be caused by brittle failure (Hajiabdolmajid et al., 2002a; Diederichs, 2002). With brittle failure, the mobilization of the frictional strength is delayed until a significant amount of the cohesive strength has been lost as a result of extension cracks. The slabbing and splitting is the result of the initiation and uninhibited growth and propagation of extension cracks into near vertical fractures at low confinement (Diederichs, 2002). At low confining stresses near the surface of an excavation, the cracks can freely propagate and interact upon crack initiation because the frictional strength is not mobilized (Hajiabdolmajid et al., 2002b). This results in the yield strength of the rock reducing to the crack initiation stress (Diederichs, 2002; Hajiabdolmajid et al., 2003). Essentially, once a crack initiates, it is free to grow and propagate in such an environment. In a more confined environment, crack propagation and growth would be restricted and yield would only occur as the amount of cracking and coalescence of the cracks was sufficient to allow for interaction between the cracks. Along the side of a limestone pillar, the confining stresses are low and the

geometry should not restrict the propagation of cracks that do initiate. Also from observations in a number of limestone mines, pillar spalling has initiated at stress levels that are about 10 percent of the uniaxial compressive strength of the rock (Esterhuizen et al 2006). Therefore, since the brittle failure criterion appears to be applicable to limestone pillars, this criterion is used in the models to determine failure. Further, brittle failure involves the failure of the intact rock and is not related to the more general rock mass strength. Therefore, the brittle failure is associated with the intact rock strength.

In this study for brittle failure, the rock strength is based on crack initiation during a uniaxial compression test. This can be about 1/3 of the uniaxial compressive strength of the intact rock. To model the brittle failure, a bilinear Mohr-Coulomb criterion is used. Brittle failure can be considered a special case of the Mohr-Coulomb criterion where the friction angle is zero. The second portion of the envelope at higher confining pressures is based on the cohesion and friction angle for the rock mass. From the intersection of these two envelopes in the maximum-minimum (σ_1 - σ_3) stress space, the confining pressure where this transition will take place in the model can be calculated. For comparison, the models were also run using a linear Mohr-Coulomb criterion with the cohesion and friction angle based on the rock mass properties.

The effects of increasing pillar length when geologic structures weaken a pillar are also examined. For these models, the Coulomb criterion of failure with a plane of weakness is utilized to determine failure (Horino and Ellickson, 1970; Jaeger and Cook, 1976). In this case, the dip of the weakness and the angle of friction and cohesion along the planes of weakness are the controlling strength parameters.

MODEL PARAMETERS

A three-dimensional finite difference code was used to model the pillars. This is the FLAC3D code version 3.0 (Itasca, 2005) The model layout and input parameters are discussed below.

Model

The basic layout and geometry used for the models is shown in figure 2. The model consisted of a main and immediate roof and a main and immediate floor above and below the pillar. The total thickness of the roof is 56 m and of the floor 64 m. The crosscuts and entries surrounding the pillar were 6 m wide (one half a 12-m roof span). For the pillar, the elements were 1 m by 1 m by 1 m cubes.

In the models, the roof and floor were fixed along the sides in the x and y directions with the floor fixed along the bottom in the vertical direction. A force (through the use of grid point velocities) was applied to the top of the model in the vertical direction, thus loading the pillar at a controlled rate until failure. The average stress across the pillar was then calculated during model loading with the peak pillar stress being captured. This average peak pillar stress is the maximum pillar strength and is used to evaluate the effects of the changes in pillar geometry.

Model Properties

The rock mass properties used in the model are based on the rock mass rating developed from 30 underground limestone mines (Esterhuizen et al., 2006). The average RMR for these mines is approximately 75, and this value was used to calculate the "s" and

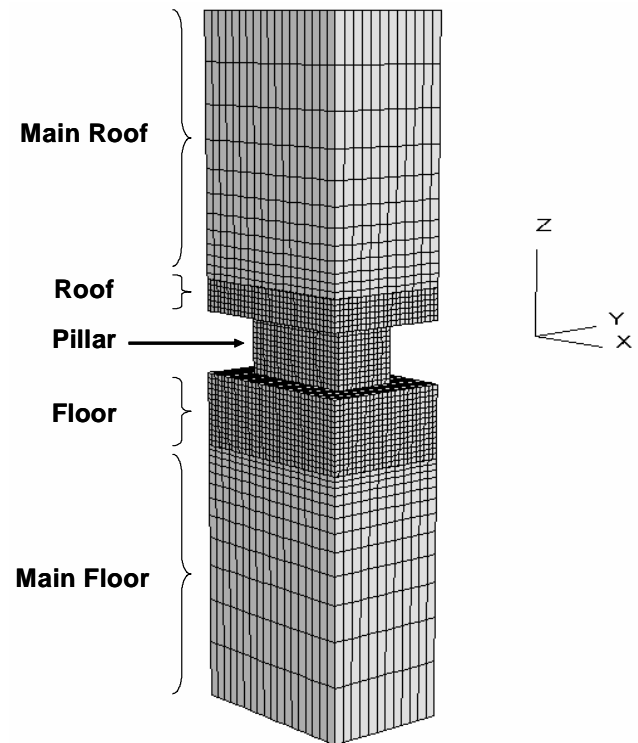


Figure 2. Basic model configuration used in the numerical modeling.

"m" parameters for the Hoek-Brown failure criteria (Hoek and Brown, 1980; Brady and Brown, 1993). These values were then converted to a friction angle and cohesion that could be used in the Mohr-Coulomb criteria (Hoek and Brown, 1997). Table 1 gives the properties used in the models for both the brittle and the Mohr-Coulomb criteria. The failure strength parameters are at zero percent plastic strain, while the values at the other levels of plastic strain are the post failure properties used in the models at that strain level. Strain softening is used to simulate the post failure performance of the elements in the pillar. The percent of plastic strain is the amount of strain after failure has occurred. These post failure properties control how fast the material strength decreases to the residual level after failure. In the models, a bulk modulus of 40 GPa and a shear modulus of 24 GPa were used for the pillar, roof and floor. Further, the roof and floor elements were not allowed to fail. The roof and floor are in this case composed of the same material as the pillar. Even if the roof and floor elements were allowed to fail, the elements are more confined than the pillar elements and the pillar would fail first thus reducing the stress in the roof and floor resulting in the roof and floor elements never reaching the failure stress. Not allowing the roof and floor elements to fail reduces the model run times.

For the brittle failure, an intact uniaxial compressive for the limestone of 150 MPa was used. The brittle pillar compressive strength was then taken as 1/3 of this value or 50 MPa. Again this value is based on the assumed stress level required for crack initiation. However, for the modeling, a friction angle and cohesion must be calculated. These are calculated for the brittle failure using the Mohr-Coulomb criteria, the brittle failure uniaxial compressive strength and a friction angle of zero. With the brittle failure, above a certain confining stress, the Mohr-Coulomb criterion based on the rock mass properties is used. This necessitates a bilinear model for the brittle failure. Figure 3 shows

Table 1. Peak and post failure strength properties used in models for the different failure criteria. Peak properties are at zero percent plastic strain.

Property	Plastic Strain					
	0	0.001	0.002	0.005	0.01	0.02
Brittle Failure						
Cohesion, MPa	25	-	-	5	1.25	-
Tension, MPa	2.7	0	-	-	-	-
Friction Angle, deg	0	-	-	-	-	-
Dilation, deg	30	-	-	-	0	-
Mohr-Coulomb Failure						
Cohesion, Mpa	8.1	-	-	-	2.43	0.8
Tension, Mpa	2.7	0	-	-	-	-
Friction Angle, deg	47.6	-	-	-	-	-
Dilaton, deg	30	-	-	-	0	-
Ubiquitous Joints						
Jcohesion, MPa	1	0.2	-	-	-	0
Jtension, MPa	0.4	0	-	-	-	-
Jfriction Angle, deg	42	-	30	-	-	-
Jdilation, deg	0	-	-	-	-	-

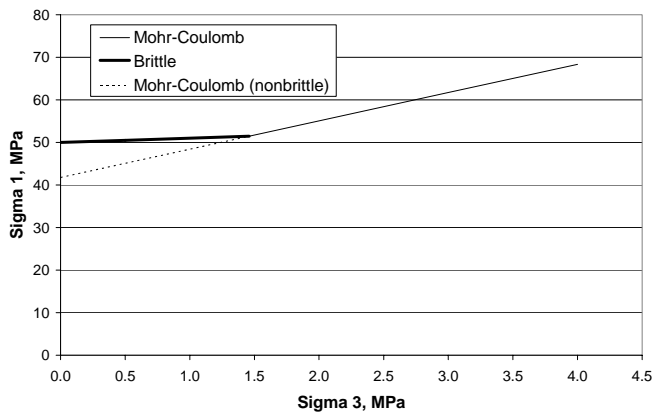


Figure 3. Mohr-Coulomb and bilinear brittle failure criteria as used in the numerical models.

the bilinear brittle Mohr-Coulomb criterion and the Mohr-Coulomb criterion for the rock mass.

Geologic structures were modeled using the ubiquitous joint feature in FLAC3D. The properties of the ubiquitous joints are also given in table 1. In these models, the failure may occur along the joints or through the solid rock or the rock mass. Where failure occurs in the rock or rock mass the bilinear brittle failure criteria is used. The dip angle for the planes of weakness was taken as 60 degrees from the horizontal. Again, strain softening is used to develop the post failure behavior of the elements in the pillars.

PARAMETRIC DESIGN

In this investigation both the pillar length and model failure criteria were varied. The criteria included brittle, Mohr-Coulomb or a ubiquitous joint failure. The ubiquitous joint models were used to evaluate the effects of geologic structure that could

significantly reduce the pillar strength and be a factor at relatively shallow depths. The brittle and Mohr-Coulomb failure criteria were used to evaluate the conditions where the pillar stress is sufficient to cause pillar failure.

For each of these failure criteria, the pillar width-to-length ratio was varied as was the pillar width-to-height ratio. In all cases, the pillar width was 12 m. Table 2 shows the pillar heights and lengths used in the models for a given failure criteria. The base case in each series is a square pillar.

Table 2. Experimental matrix for modeling of limestone pillar strengths. All pillars had a width of 12 m.

Length-to-width ratio	Width-to-height ratio				
	0.5	0.66	1	1.2	1.5
Brittle Failure					
1	x	x	x	x	x
2	x	x	x	x	x
3	x	x	x	x	x
4	x	x	x	x	x
5					x
6					x
Mohr-Coulomb Failure					
1	x	x	x	x	x
2	x	x	x	x	x
3	x	x	x	x	x
4	x	x	x	x	x
5			x	x	x
6			x	x	x
Ubiquitous Joint Failure, joint strike 90° to long axis of pillar					
1	x	-	x	-	x
2	x	-	x	-	x
3	x	-	x	-	x
Ubiquitous Joint Failure, joint strike 0° to long axis of pillar					
1	x	-	x	-	x
2	x	-	x	-	x
3	x	-	x	-	x

For the ubiquitous joint models, the direction of the strike of the planes of weakness was either 0 or 90 degrees to the long axis of the pillars. For a 0-degree orientation, the strike of the joints was parallel to the long axis of the pillar and for a 90-degree orientation, the strike of the joints was perpendicular to the long axis of the pillar.

MODEL RESULTS

The parameter used to determine the effects of pillar length on the pillar strength was the average vertical stress on the pillar at failure. This stress is the maximum pillar strength for the conditions. The strength of the square pillar at a width of 12 m is then used as a baseline to evaluate the increase in pillar strength with length. Table 3 shows the maximum pillar strength of the model pillars for brittle and Mohr-Coulomb failure criteria and for both joint orientations for the ubiquitous joint models.

Table 3. Pillar strengths determined from models for different pillar geometries and failure criteria.

Width-to-length ratios	Width-to Height Ratio				
	0.5	0.66	1	1.2	1.5
Pillar Strength, MPa					
Brittle Failure					
1	49.6	51.6	74.1	89.4	105.8
2	49.4	58	78.4	100.5	121.1
3	49.3	59.6	78.5	111	126.3
4	49.1	60.6	79	112	139.1
5	-	-	-	-	156.4
6	-	-	-	-	157.5
Mohr-Coulomb Failure					
1	43.7	52.4	80.5	101.3	127.6
2	45.7	59.2	101	124.1	147.3
3	46.1	61.2	107.9	133.5	155.6
4	46.3	62.3	111.9	137.7	163.3
5	-	-	114.5	140.3	168.4
6	-	-	116	142.1	170.8
Ubiquitous Joint Failure, 90° to long axis of pillar					
1	4.7	-	39	-	62.8
2	24.8	-	59.8	-	91.2
3	34.5	-	69.3	-	103
Ubiquitous Joint Failure, 0° to long axis of pillar					
1	4.8	-	39	-	62.8
2	4.8	-	40.6	-	68
3	4.7	-	40.6	-	70.6

Figure 4 shows the maximum pillar strength versus the pillar length for both the brittle and Mohr-Coulomb failure criteria for each pillar height. The maximum pillar strengths occur with the pillars with the largest width-to-height ratios and the longest lengths for both failure criteria. In general, the pillar strength does increase with pillar length, although this depends on the pillar width-to-height ratio. For the slenderest pillars with a width-to-height ratio of 0.5, there is no increase in strength with length with brittle failure and only a small increase in strength with the Mohr-

Coulomb failure. Further, with increasing length, the rate at which the pillars gain strength decreases for both failure criteria.

Figure 5 shows the pillar strength versus the pillar length for each pillar height for the ubiquitous joint models for both joint orientations. When the strike of the joint system is perpendicular to

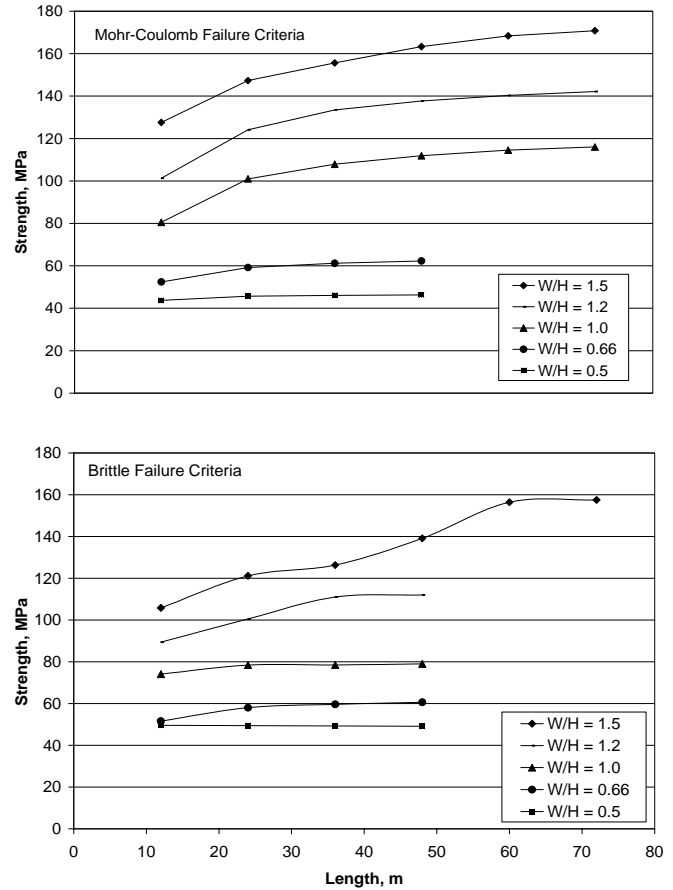


Figure 4. The strength increase with pillar length for various pillar width-to-height ratios for the Mohr-Coulomb failure criteria (top) and for the brittle failure criteria (bottom).

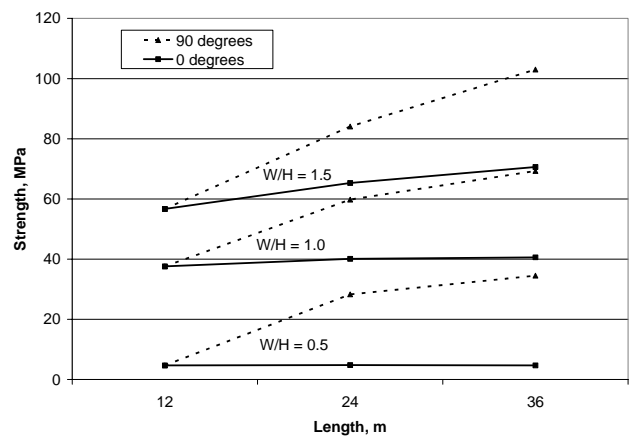


Figure 5. The strength increase with pillar length for various pillar heights with ubiquitous joints either perpendicular (90 degrees) or parallel (0 degrees) to the long pillar axis.

the long axis of the pillar, there is clearly an increase in the pillar strength with pillar length. Again, the rate of increase in pillar strength decreases with the length. However, when the structures strike is parallel with the long axis of the pillar there is a much smaller increase in strength with length for the squat pillars and little or no increase in pillar strength with length for the slender pillars.

PILLAR STRENGTH EQUATIONS BASED ON GEOMETRY

Clearly, there is interaction between the pillar width-to-height and width-to-length ratios for both the brittle and Mohr-Coulomb failure with the dominant parameter being the width-to-height ratio (table 3, figure 4). Further, the contribution of the length in increasing the strength diminishes with increasing length. Therefore, any equations that are developed for the pillar strength must reflect this interaction and the diminishing effects of length. The following equations were developed for these two failure criteria based on a multiple regression analysis of the data. The dependent variable in the regression analysis was the ratio of the pillar strength to the pillar strength for a square pillar with a width-to-height ratio of one.

For the brittle failure criteria the following equation was developed

$$C_{Rbf} = C_{S1}(1.51(W/H) + 0.46(W/L) - 0.78(W/H)(W/L) - 0.18) \quad (1)$$

where: C_{Rbf} = compressive strength with brittle failure for a given pillar width and length,
 C_{S1} = compressive strength for a pillar with a width-to-height to length ratio of 1.0,
 W = pillar width,
 H = pillar height, and
 L = pillar length.

The multiple correlation coefficient squared for this regression is 0.96.

For the Mohr-Coulomb failure criteria, the following equation was developed

$$C_{Rmc} = C_{S1}(1.64(W/H) + 0.15(W/L) - 0.58(W/H)(W/L) - 0.18) \quad (2)$$

where: C_{Rmc} = compressive strength with Mohr-Coulomb for a given pillar width and length.

The multiple correlation coefficient squared for this regression is 0.99. The correlation coefficients of both these equations are very high. However, the equations are based on modeled pillars with the range of width-to-height ratios from 0.5 to 1.5 and width to length ratios from 1.0 to 6.0. Therefore, the application of these equations should be limited to those ranges.

Figure 6 shows a graph of the ratio of the rectangular to square pillar strength versus the pillar length-to-width ratio for different width-to-height ratios developed from both these equations. For the brittle failure criteria, there is a large difference in the gain in pillar strength with length depending on the width-to-height ratio of the pillar. An increase in strength of over 40 percent occurs for the squattest pillar. For a width-to-height ratio of 0.6, the strength ratio is nearly one for length-to-width ratios from one to six. Essentially there is no increase in pillar strength with length for width-to-height ratios less than 0.6. Therefore, the brittle failure equation is not valid for ratios that are below 0.6 since there is no change in

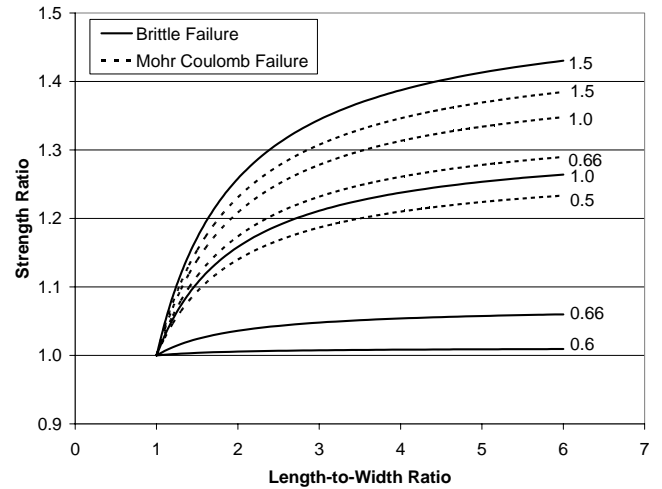


Figure 6. The ratio of a rectangular to a square pillar strength versus the pillar length-to-width ratio for various pillar width-to-height ratios from equations developed from both the brittle failure and Mohr-Coulomb failure criteria.

strength for more slender pillars. Based on the models results, the width-to-height ratio where there is no further increase in strength with length occurs between 0.5 and 0.66. Therefore, for the slender pillars with width-to-height ratios of about 0.66 and below, there is little increase in the pillar strength with length.

For the Mohr-Coulomb failure criteria, the change in the strength ratio for a similar range of width-to-height ratios is much less than with brittle failure. This results in part from a much lower coefficient for the independent width to length term in the equation. With the squattest pillar, the strength ratio is just under that for the brittle failure. There is also an increase in pillar strength with length with the most slender pillar as compared to no strength increase when the same pillar is subject to brittle failure. Even though there is some increase in pillar strength with length for pillars with a width-to-height ratio of 0.5, the amount of the strength increase is small because of the reduced pillar strength for these slender pillars.

For the more slender pillars with width-to-height ratios from 1 to 0.66 (12- and 18-m-high pillars) with brittle failure and with a width-to-height ratio of 0.66 for the Mohr-Coulomb failure, there is some strength gain from a square pillar to a rectangular pillar with a length-to-width ratio of two, but little increase in strength for a pillar with a length-to-width ratio of three. Essentially, for pillars with these width-to-height ratios there is no benefit of increased pillar strength beyond a pillar length-to-width ratio of two. In general for both failure criterion, with width-to-height ratios below one, ratios that will occur with benching, the benefits of length on pillar strength diminish rapidly especially beyond a length-to-width ratio of two. With the benching, as the pillar width-to-height ratio reaches 0.5, all gains in strength from the pillar length are essentially lost.

Of these two criteria used in the modeling, the brittle failure criterion is probably more relevant to use in the underground limestone mines because of the type of failure that could be expected. Therefore, the brittle failure equation will probably give more representative pillar strengths when rectangular pillars are used in underground limestone mines. The brittle failure equation can also account for the lack of strength increase with length in the most slender pillars, while the Mohr-Coulomb equation does not.

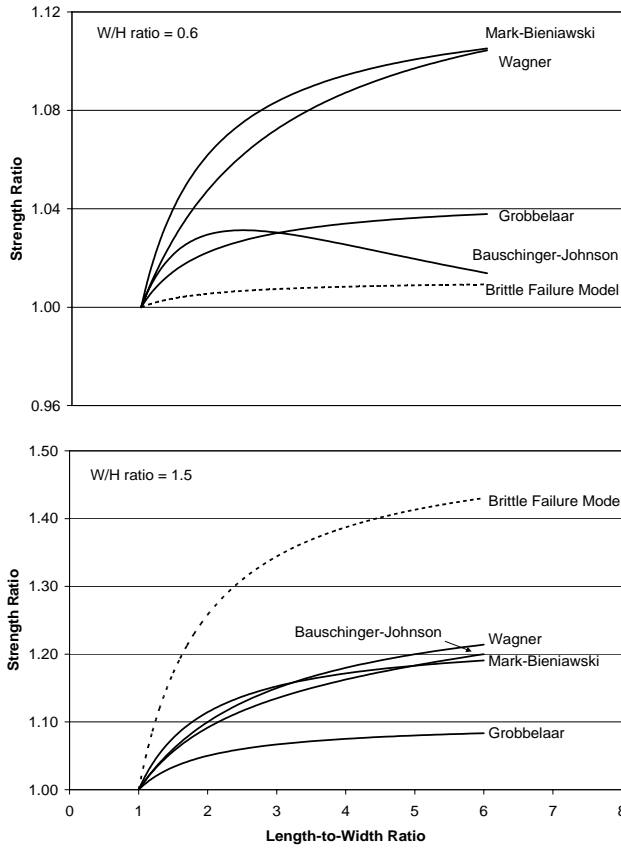


Figure 7. The ratio of a rectangular to square pillar strength versus the length-to-width ratio for the pillar comparing the brittle failure pillar equation to other pillar equations used to estimate the strength of rectangular pillars (Babcock, 1994; Mark and Chase, 1997; Mark 1999; Salamon, 1983).

The results of the equation for the brittle failure can be compared to the four published equations discussed in the background section. Figure 7 shows a comparison of these equations for two pillar width-to-height ratios. For the squat pillar, the brittle failure equation predicts larger strength increases with pillar length than the other equations. However, for the slender pillar, the brittle failure equation is the only equation that predicts little or no increase in pillar strength with pillar length.

BASIS FOR INCREASE IN PILLAR STRENGTH WITH LENGTH

The increases in the pillar strength with the change in length can be evaluated in terms of the pillar geometry. In this case the geometry of interest is the relationship between the areas affected by the pillar ends to the total area of the pillar. Figure 8 shows a pillar separated into the areas affected by the ends of the pillar and a central portion of the pillar length not affected by the ends. Essentially, there is a central portion of the pillar length that behaves as if there were no pillar ends.

Based on figure 8 the following equation can be developed for the relationship between the strength of a square and rectangular pillar;

$$C_R = C_S + F_c (1 - A_e/A_p) \quad (3)$$

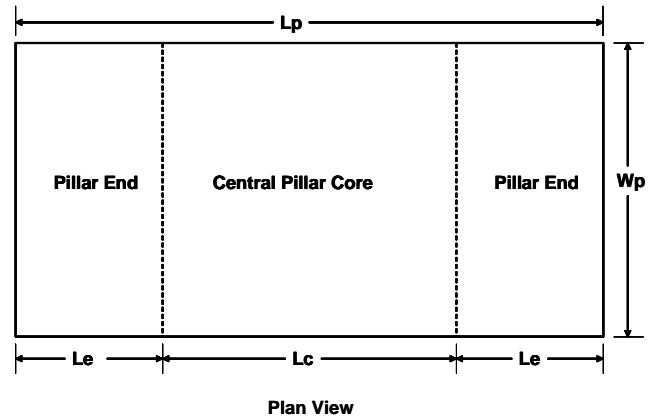


Figure 8. Relationship of the dimensions of a pillar, the central pillar core and the pillar ends where L_p = length of pillar, W_p = width of pillar, L_c = length of central pillar core and L_e = length of pillar ends.

- where: C_R = compressive strength of a rectangular pillar,
 C_S = compressive strength of a square pillar,
 F_c = confining stress factor,
 A_e = area of the ends of the pillar, and
 A_p = area of the pillar.

Essentially, there is a central pillar core that is more confined than the ends of the pillars, and will therefore carry more stress at peak pillar strength than the ends. A higher percent of the pillar in the central region results in higher pillar strengths.

For the Mark-Bieniawski rectangular pillar equation, from geometric considerations, the pillar stress distribution is calculated based on end effects that are one half the pillar width (Mark and Chase 1997). If the length of the pillar in an end area is assumed to be equal to one half of the pillar width (6 m), the ratio of the pillar end area to the pillar area for the different lengths of modeled pillars are 1.0 for the 12 m pillar, 0.5 for the 24 m pillar, 0.33 for the 36 m pillar, 0.25 for the 48 m pillar, 0.2 for the 60 m pillar, and 0.17 for the 72 m pillar. These ratios can then be used to calculate the confining stress factor for each of the modeled pillar results using equation 3 since the compressive strengths for the square and rectangular pillars are known for a given geometry (table 3). Table 4 shows the calculated confining stress factors. For pillars that are 12 m or higher, the stress factor for either failure criteria does not vary significantly with pillar length. For these slender pillars, the change in the ratio of the area of the ends to the pillar area can explain the increase in pillar strength.

This is not the case for the squattest pillar. The confining stress factor increases significantly above a pillar length of 36 m for both types of failure. Not only is ratio of the area of the ends to the total pillar area of importance, but also that the ends are significantly reducing the confinement along a portion of the length of the pillar. This may be occurring in the more slender pillars but can not be observed in the pillar strength because the pillar performance is dominated by the pillar height. However, the increase in the confining stress is limited to a transition from a square to a rectangular pillar that appears to be completed with a 60-m pillar length.

Table 4. Confining stress factor calculated for each failure criteria.

Width-to-Length Ratio	Width-to-Height Ratio			
	0.5	0.66	1	1.5
Brittle Failure -Confining Stress, MPa				
2	0	8.6	12.8	30.6
3	0	6.6	11.9	30.5
4	0	6.5	12	44.4
5	-	-	-	63.3
6	-	-	-	62.3
Mohr-Coulomb Failure-Confining Stress, MPa				
2	4	13.6	41	39.4
3	3.6	13.1	40.9	41.8
4	3.5	13.2	41.9	47.6
5	-	-	42.5	51
6	-	-	-	52

The reduction in confinement along a portion of the length of the squattest pillar can be seen with the brittle failure with the depth of brittle failure depending on confinement. The depth of brittle failure will be less with higher confinement. For the square, 8-m-high pillar, the depth of brittle failure is 2 m around the entire pillar. For the 24-m-long pillar, the depth of brittle failure is only one meter along the middle third of the pillar and 2 m deep along each third of the pillar at the ends. For the 60-m-long pillar, the depth of failure is only 1 meter along the middle two thirds of the pillar and 2 m deep along the remaining pillar ends.

For the most slender pillars with a width-to-height ratio of 0.5, there is little or no change in strength with increasing length. For the brittle failure, the yield stress is the peak pillar strength with a rapid collapse in pillar strength after yield. Figure 9 shows stress-strain curves for a 24 m high pillar with a 36 m length for both brittle and Mohr-Coulomb. Essentially, with brittle failure there is no confinement that develops in the pillar at peak pillar strength. With the Mohr-Coulomb failure, the confinement is sufficiently small such that any decrease in the end effects with length makes only a small difference in the pillar strength. Essentially pillar height dominates the pillar behavior.

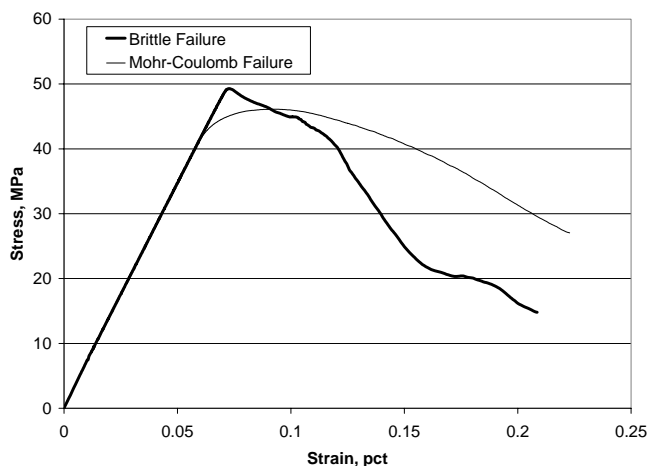


Figure 9. Stress-strain curves for a 24 m high pillar with a 36 m length for both brittle and Mohr-Coulomb failures.

GEOLOGIC STRUCTURE

For geologic structure in the form of ubiquitous joints, there is a significant reduction in pillar strength compared to non-jointed pillars with the same geometry. The amount of this reduction depends on the pillar geometry as well as the orientation of the joints. However, the largest reduction in strength occurs with the most slender pillars.

For the jointed pillars, the pillar geometry and orientation of the geologic structure also have a significant effect on the jointed pillar strength. A longer pillar significantly increases the pillar strength when the joint strike is orientated perpendicular to the long axis of the pillar. Essentially, the joints are daylighted at the ends thus weakening the ends of the pillar but leaving a central core that depends on the general rock mass or intact rock strength. With increasing pillar length, the size of this central core increases and thus increasing the strength. Therefore, to improve the pillar strength in the presence of geologic structure, the amount of the pillar that is not affected by a daylighted structure must be sufficient. It should be noted that joint dip, in this case 30 degrees from vertical will affect the amount of the central pillar core that can develop. For the most slender pillar with a width-to-height ratio of 0.5, a very large increase in strength occurs from a square pillar to a rectangular pillar with a length-to-width ratio of 2. The joints are daylighted across the entire square pillar, completely controlling the pillar strength resulting in a very weak pillar. Thus, when a central pillar core develops with an increase in length, there is a significant gain in strength.

If the strike of the joints or structure is parallel to the long pillar axis, significant improvement in the pillar strength only occurs with the squattest pillars. For a slender pillar with a width-to-height ratio of 0.5, there is no increase in strength as a result of the structure daylighting through both the square and rectangular pillars. However, significant gains in the pillar strength can be achieved where joints or structure are orientated perpendicular, rather than parallel, to the long axis of the pillar.

CONCLUSIONS

The effects of increased pillar length on pillar strength for pillars in limestone mines was investigated using numerical modeling. Based on the results of the modeling, several conclusions can be developed.

For the failure of the rock and rock mass without specific geologic structures, two failure criteria were examined in the models: a Mohr-Coulomb and a brittle failure criterion. Thus, two different pillar design equations involving the pillar length were developed from a regression analysis of the modeling results. However, because of the nature of limestone mine and pillar geometry and the type of expected pillar failure, the equation based on the brittle failure criteria is the one most relevant to estimating rectangular limestone pillar strengths.

For the pillar strength equation involving brittle failure, the effects of length vary with the width-to-height ratio of the pillar. Below a width-to-height ratio of about 0.66, there is little or no increase in strength with length. At these slenderness ratios, there is little or no confinement across the pillar at peak strength. Only with the more squat pillars is there a significant gain in strength with pillar length.

With brittle failure and width-to-height ratios of one or less, there is little or no increase in the pillar strength with length especially beyond a length-to-width ratio of two. As a result, if rectangular pillars are used with benching, as the width-to-height ratio drops below one, the benefits of increased pillar strength from pillar length will be lost.

The effects of pillar length on strength as determined by the equation using the Mohr-Coulomb failure criteria is not as dependent on the pillar width-to-height ratio as with the brittle failure. However, with very slender pillars there is only a limited amount of confinement; therefore the gain in strength is also small. Based on either equation, there is little benefit to be gained in pillar strength with increased length for slender pillars.

The gain in pillar strength with length for the more slender pillars can be explained by the geometry of the pillar. The geometry that determines the strength increase is the ratio of the area of the pillar affected by the ends to the area of the pillar resulting in the rate of increase in strength diminishing with length. For the squattest pillar, the change in strength is also affected by an increase in pillar confinement along the central length of the pillar as the pillar transitions from a square to a long rectangular pillar.

Where geologic structure can weaken a pillar and the structure is daylighted, additional pillar length can significantly increase the pillar strength. In general, however, the greatest gain in pillar strength is obtained when the strike of the geologic structure is orientated 90-degrees to the long axis of the pillar. Essentially, with length, the core area of the pillar not affected by the structure increases, thus resulting in a gain in pillar strength.

REFERENCES

- Babcock, C. (1994). Critique of Pillar Design Equations from 1833 to 1990. U.S. Department of the Interior, Bureau of Mines IC 9398.
- Brady, B.H.G., Brown, E.T. (1993). Rock Mechanics for Underground Mining. Second Edition. Kluwer Academic Publishers, Dordrecht, The Netherlands, 571 pp.
- Diederichs, M. (2002). Stress Induced Damage Accumulation and Implications for Hard Rock Engineering. NARMS-TAC, University of Toronto, pp. 3-12.
- Esterhuizen, G.S., Iannacchione, A.T., Ellenberger, J.L. and Dolinar, D.R. (2006). Pillar Stability Issues Based on a Survey of Pillar Performance in Underground Limestone Mines. Proceedings of the 25th International Conference on Ground Control in Mining Morgantown, WV, Aug 1-3, pp. 354-361.
- Grau III, R.H., Mucho, T.P., Robertson, S.B., Smith, A.C. and Garcia, F. (2002). Practical Techniques to Improve the Air Quality in Underground Stone Mine. Proceedings of the North American/Ninth U.S. Mine Ventilation Symposium, Kingston, Ontario, Canada, June 8-12, pp. 123-129.
- Grau III, R.H., Krog, R.B. and Robertson, S.B. (2006). Maximizing the Ventilation of Large-Opening Mines. Proceedings of the 11th U.S./North American Mine Ventilation Symp., University Park, PA, June 5-7.
- Hajiabdolmajid, V., Kaiser, P.K. and Martin, C.D. (2002a). Mobilization of Strength in Brittle Failure of Rock-in Laboratory vs. In Situ. NARMS-TAC, University of Toronto, pp. 227-234.
- Hajiabdolmajid, V., Kaiser, P.K. and Martin, C.D. (2002b). Modeling Brittle Failure of Rock. Intl J of Rock Mechanics and Mining Sciences 39:731-741.
- Hajiabdolmajid, V., Kaiser, P.K. and Martin, C.D. (2003). Mobilised Strength Components in Brittle Failure of Rock. Geotechnique 53(3):327-336.
- Hoek, E. and Brown, E.T. (1980). Underground Excavations in Rock. The Institutions of Mining and Metallurgy, London, 527 pp.
- Hoek, E., Brown, E.T. (1997). Practical Estimates of Rock Mass Strength. Intl J of Rock Mechanics and Mining Sciences, 34:1165-1186.
- Horino, F.G., Ellickson, M.L. (1970). A Method for Estimating Strength of Rock Containing Planes of Weakness. U.S. Department of the Interior, Bureau of Mines RI 7449.
- Iannacchione, A.T., Coyle, P.R. (2002). An Examination of the Loyalhanna Limestone's Structural Features and Their Impact on Mining and Ground Control Practices. Proceedings of the 21st International Conference on Ground Control in Mining Morgantown, WV, Aug 6-8, pp. 218-227.
- Iannacchione, A.T., Marshall, T.E., Burke, L.M., Melville, R. and Litsenberger, J. (2003). Safer Mine Layouts for Underground Stone Mines Subjected to Excessive Levels of Horizontal Stress. Min Eng (4):25-31.
- Iannacchione, A.T. (1999). Analysis of Pillar Design Practices and Techniques for U. S. Limestone Mines. Trans Inst Min Metall, Vol. 108, A152-160.
- Itasca Consulting Group (2005). FLAC3D, Fast Lagrangian Analysis of Continua in 3-Dimensions, version 3.0. Minneapolis, MN.
- Jaeger, J.C. and Cook, N.G.W. (1976). Fundamentals of Rock Mechanics. John Wiley & Sons, Inc., New York, 583 pp.
- Mark, C. (1990). Pillar Design Methods for Longwall Mining. U.S. Department of the Interior, Bureau of Mines IC 9247.
- Mark, C. and Chase, F.E. (1997). Analysis of Retreat Mining Pillar Stability (ARMPS). Proceedings of the New Technology for Ground Control in Retreat Mining. U.S. Department of Health and Human Services, National Institute for Occupational Safety and Health (NIOSH), IC 9446, pp 17-34.
- Mark, C. (1999). Empirical Methods for Coal Pillar Design. Proceedings of the Second International Workshop on Coal Pillar Mechanics and Design. U.S. Department of Health and Human Services, National Institute for Occupational Safety and Health (NIOSH), IC 9448, pp. 145-154.
- Roberts, D.P., Ryder, J.A. and van der Merwe, J.N. (2005). Development of Design Procedures for Long Slender Pillars. Final Report Task 2.14, Coaltech 2020, March 11, 65 pp.

Salamon, M.D.G. (1983). The Role of Pillars in Mining. The South African Institute of Mining and Metallurgy Monograph Series No. 5, Rock Mechanics in Mining Practice, The South African Institute of Mining and Metallurgy, pp. 173-200.

Stacey, T.R. and, Yayhavan, K. (2003). Examples of Fracturing of Rock at Very Low Stress Levels. ISRM-Technology Roadmap for Rock Mechanics; South African Institute of Mining and Metallurgy, pp. 1155-1159.